Diffusion-Weighted Imaging with Learned Nonlinear Latent Space Modeling and Self-Supervised Reconstruction (DeepDWI)

Zhengguo Tan, Julius Glaser, Patrick A Liebig, Annika Hofmann, Frederik B Laun, Florian Knoll

***Abstract*—The code is publicly available at: `https://github.com/ZhengguoTan/DeepDWI`.**

***Index Terms*—Diffusion-weighted imaging, Image reconstruction, Generative AI, Latent space, Self-supervised learning**

I. Introduction

HIGH-dimensional magnetic resonance imaging (HD-MRI) has been a flourishing field, which refers to the acquisition, reconstruction and analysis of multi-dimensional multi-contrast-weighted MRI data. Examples of HD-MRI include but are not limited to magnetic resonance spectroscopic imaging (MRSI) [1], diffusion-weighted imaging (DWI) [2], [3], and quantitative parameter mapping [4], [5]. Conventional HD-MRI, however, necessitates long acquisition, resulting in data vulnerable to subject motion and system imperfections, as well as high computational burden. DWI, in particular, poses challenges in the pursuit of high spatial, temporal, and angular resolution. DWI is typically acquired via the pulsed gradient spin echo sequence [6] followed by fast echo-planar imaging (EPI) readouts [7]. However, the use of long echo trains in EPI results in geometric distortion artifacts and low spatial resolution. Plus, the interest in acquiring multiple diffusion directions for the improvement of angular resolution and for the probe to tissue microstructure increases the scan time.

This work was supported in part by German Research Foundation (DFG) under projects 513220538 and 512819079, project 500888779 in the Research Unit RU5534 for MR biosignatures at UHF, and by the National Institutes of Health (NIH) under grants R01 EB024532 and P41 EB017183. In addition, scientific support and HPC resources were provided by the Erlangen National High Performance Computing Center (NHR) of Friedrich-Alexander-University Erlangen-Nuremberg (FAU) under the NHR project b143dc. NHR is funded by federal and Bavarian state authorities. NHR@FAU hardware is partially funded by DFG under project 440719683. *(Corresponding Author: Zhengguo Tan)*

Z. Tan was with the Department Artificial Intelligence in Biomedical Engineering (AIBE), FAU, Erlangen, Germany. He is now with the Michigan Institute for Imaging Technology and Translation (MIITT), Department of Radiology, University of Michigan, Ann Arbor, MI 48109 USA (e-mail: zgtan@med.umich.edu).

J. Glaser was with the Department of Medical Engineering, FAU, Erlangen, Germany. He is now with the Institute of Radiology, University Hospital Erlangen, FAU, Erlangen, Germany (e-mail: julius.glaser@fau.de).

P. A. Liebig is with Siemens Healthcare GmbH, Erlangen, Germany (e-mail: patrick.liebig@siemens-healthineers.com).

A. Hofmann is with the Department AIBE, FAU, Erlangen, Germany (e-mail: annika.ah.hofmann@fau.de).

F. B. Laun is with the Institute of Radiology, University Hospital Erlangen, FAU, Erlangen, Germany (e-mail: Frederik.Laun@uk-erlangen.de).

F. Knoll is with the Department AIBE, FAU, Erlangen, Germany (e-mail: florian.knoll@fau.de).

Advances in parallel imaging [8]–[12] and compressed sensing [13]–[15] have enabled accelerated acquisition for HD-MRI. In particular, the low-rank model [16] has been a powerful tool in dimension reduction. Usually, singular value decomposition (SVD) is used to learn a truncated temporal basis function from a large-scale physics-informed dictionary [17]–[19]. The temporal basis function is then integrated with the MRI forward model, i.e. the sensitivity encoding operator [11], for joint reconstruction of the corresponding spatial basis images. In addition, low-rank regularization can be employed in the joint reconstruction [20].

Beyond the low-rank technique, advanced neural networks, e.g. autoencoder [21], have been explored for HD-MRI reconstruction and proven to supply more accurate representations of high-dimensional data than SVD. Lam et al. [22] and Mani et al. [23] proposed to first learn a denoising autoencoder (DAE) model from a physics-informed simulated dictionary and then incorporate the learned DAE model as a regularizer in the alternating direction method of multipliers (ADMM) [24] unrolling reconstruction. Pioneered by Gregor and LeCun [25], algorithm unrolling enables the use of learned deep *prior* as regularization and faster inference than iterative reconstruction with hand-crafted regularization functions [26]. Algorithm unrolling has been introduced to accelerated MRI reconstruction and employed in various scenarios: supervised learning with fully sampled reference images [27], [28], and self-supervised learning with only undersampled data available for training [29], [30]. Noteworthy, it is rather difficult to acquire fully-sampled DWI for the training of a regularization functional. First, fully-sampled DWI requires a longer echo train in EPI, which not only elongates the scan time but also increases off-resonance-induced geometric distortion. Second, there exists a wide range of diffusion acquisition modes, thereby requiring a larger dataset than the two-dimensional imaging scenario [31]. Therefore, self-supervised learning is more appropriate for DWI reconstruction.

Deep neural networks are capable of learning not only regularization functions, but also MR-physics forward operators. Liu et al. [32] proposed the reference-free T_1 parameter maps extraction (RELAX) self-supervised deep learning reconstruction, which learns the mapping from T_1 parameter maps to undersampled multi-coil multi-contrast k-space data. Arefeen et al. [33] proposed to replace the conventional SVD-based

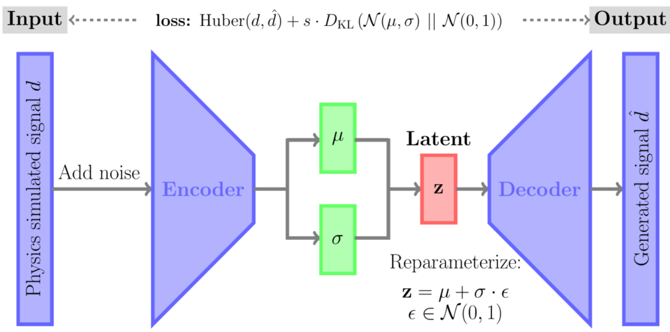

Fig. 1. The architecture of a variational autoencoder.

linear subspace modeling [17] by the latent decoder model within DAE for improved T_2-weighted image reconstruction. The capability of DAE to learn DWI models, however, is open to questions. DAE is composed of sequential fully connected layers with nonlinear activation functions. This simple architecture may fail to learn complicated functions. DWI signal is such an example. The standard diffusion tensor model [34] consists of six tensor elements, and forms DWI signals based on the multiplication of exponential functions.

In this work, we aim to develop a generalized DWI reconstruction framework with learned nonlinear latent space modeling and self-supervised reconstruction, dubbed DeepDWI.

Contributions:

- We VAE
- We ADMM unrolling for zero-shot self-supervised learning
- We 0.7 mm isotropic mesoscale resolution DWI

II. Related Work

A. Multi-Band Multi-Shot DWI Acquisition & Modeling

Our previous work [35] demonstrated the joint k-q-slice forward operator for multi-band multi-shot NAViEPI DWI acquisition. This operator can be understood as an extended sensitivity encoding (SENSE) operator [11], which maps the multi-slice multi-diffusion-weighted images ($\tilde{\mathbf{x}}$) to their corresponding k-space,

$$\mathcal{A}(\tilde{\mathbf{x}}) = \mathbf{P \Sigma \Theta F S \Phi} \tilde{\mathbf{x}} \tag{1}$$

Here, the images $\tilde{\mathbf{x}}$ are point-wise multiplied with the precomputed shot-to-shot phase variation maps ($\mathbf{\Phi}$) and coil sensitivity maps ($\mathbf{S}$). The output images are then converted to k-space via two-dimensional fast Fourier transform ($\mathbf{F}$), point-wise multiplied with the multi-band phases ($\mathbf{\Theta}$), summed along the slice dimension ($\mathbf{\Sigma}$), and then multiplied by the k-space undersampling mask ($\mathbf{P}$).

With the operator $\mathcal{A}$, the joint reconstruction reads,

$$\underset{\tilde{\mathbf{x}}}{\operatorname{argmin}} \left\| \mathbf{y} - \mathcal{A}(\tilde{\mathbf{x}}) \right\|_2^2 + \lambda \mathcal{R}(\tilde{\mathbf{x}}) \tag{2}$$

where $\mathbf{y}$ is the measured k-space data. The first term in Equation (2) presents data consistency, and the second term presents the regularization function $\mathcal{R}(\tilde{x})$ with the regularization strength λ. When using the Tikhonov regularization, i.e. $\mathcal{R}(\tilde{\mathbf{x}}) = \|\tilde{\mathbf{x}}\|_2^2$, Equation (2) can be solved via the conjugate gradient (CG) method.

B. Variational Autoencoder (VAE)

Autoencoders comprise an encoder and a decoder, connected through a latent space. Conventional autoencoders have no regularization on the latent space. Consequently, the learned latent space lacks meaningful and structural representation. To allow for dimension reduction while keeping the major part of the data structure, Kingma and Welling [36] proposed the variational autoencoder (VAE), as shown in Figure 1. In VAE, the encoder maps each diffusion-weighted signal into a Gaussian distribution ($\mathcal{N}(\mu, \sigma)$) within the latent space. The latent variable ($\mathbf{z}$) is sampled according to the encoded distribution. The decoder then maps the latent variable to the input space. The training of a VAE uses the Huber loss together with the Kullback-Leibler Divergence (KL-D). The Huber loss minimizes the difference between the input and the output, whereas KL-D minimizes the approximate posterior in latent space and the exact posterior (assumed to be Gaussian distribution).

C. Algorithm Unrolling for Deep Image Reconstruction

Algorithm unrolling has been an emerging technique in solving Equation (2) combining with deep neural networks. Algorithm unrolling consists of two ingredients. First, it learns a regularization function via deep neural networks. Second, it is constrained by the data-consistency term, i.e., the forward pass of the estimate $\mathcal{A}(\tilde{\mathbf{x}})$ must be close to the measured data $\mathbf{y}$. By mapping the operations used in iterative algorithms into networks, unrolled algorithms can be trained with data and achieve much faster inference than conventional iterative algorithms [26]. Further, recent developments have shown that the operations used in compressed sensing MRI, i.e., sparsifying transformation and soft thresholding, can be learned via neural networks. For instance, Hammernik et al. [27] proposed to unroll the gradient descent algorithm with a learned neural network (e.g. U-net [37]) as the regularization function. Aggarwal et al. [28] proposed to unroll the alternating minimization algorithm with a learned residual denoising network [38] as regularization.

D. Self-Supervised Learning for Image Reconstruction

It is difficult to acquire fully-sampled data for supervised learning in many MRI applications, e.g., dynamic imaging and diffusion-weighted imaging. To address this challenge, Yaman et al. [29] proposed self-supervised learning via data undersampling (SSDU), which learns the regularization function in Equation (2) by splitting available undersampled data into two disjoint sets, one of which is used in the data consistency term and another used for the training loss function. The training of SSDU requires large undersampled data sets. To close the domain gap between training and test data, Yaman et al. [30] proposed scan-specific zero-shot self-supervised learning (ZSSSL), which splits a single data set into three disjoint sets for the data consistency term and the loss calculation during training, and for validation, respectively. ZSSSL has been adopted for multi-contrast image reconstruction [39].

TABLE I
NAViEPI ACQUISITION PROTOCOLS

Protocol	#1	#2
Diffusion mode	MDDW	
Diffusion scheme	monopolar	
Diffusion direction	20	
b-value ($\mathrm{s/mm^2}$)	1000	
b_0	1	
FOV ($\mathrm{mm^2}$)	200	
Matrix size	200×200	286×286
In-plane resolution ($\mathrm{mm^2}$)	1.0×1.0	0.7×0.7
Slice thickness (mm)	1.0	0.7
Slices	141	176
Navigator	No	Yes
Shots	4	3
TR (ms)	7700	16200
TE (ms)	67	58/98.3
ESP (ms)	1.02	1.17
Bandwidth (Hz/Pixel)	1086	972
Partial Fourier	6/8	5/8
Acceleration	1×3	2×2
Acquisition (min)	$10:42$	$17:30$

III. Methods

A. Data Acquisition

Table I lists two acquisition protocols implemented on a clinical 7 T MR system (MAGNETOM Terra, Siemens Healthineers, Erlangen, Germany) with a 32-channel head coil (Nova Medical, Wilmington, MA, USA) and the XR-gradient system (maximum gradient strength $80\,\mathrm{mT/m}$ and a peak slew rate $200\,\mathrm{T/m/s}$). The first protocol employed in-plane fully-sampled four-shot EPI and thus supplied ground truth data for the validation of our proposed methods. The second protocol implemented mesoscale $0.7\,\mathrm{mm}$ isotropic resolution based on NAViEPI with both in-plane and slice acceleration as 2. Two volunteers with written informed consent approved by the local ethics committee participated in this study.

B. Image Reconstruction via ADMM Unrolling

We employed the ADMM unrolling to solve the self-supervised learning reconstruction in Equation (2). The update rule of ADMM unrolling reads

$$\begin{cases} \tilde{\mathbf{x}}^{(k+1)} = \underset{\mathbf{x}}{\operatorname{argmin}} \, \|\mathbf{y} - \mathcal{A}(\mathbf{x})\|_2^2 + \rho/2 \left\| \mathbf{x} - \mathbf{v}^{(k)} + \mathbf{u}^{(k)} \right\|_2^2 \\ \mathbf{v}^{(k+1)} = (\lambda/\rho) \cdot \mathcal{D}_\omega(\tilde{\mathbf{x}}^{(k+1)} + \mathbf{u}^{(k)}) \\ \mathbf{u}^{(k+1)} = \mathbf{u}^{(k)} + \tilde{\mathbf{x}}^{(k+1)} - \mathbf{v}^{(k+1)} \end{cases} \tag{3}$$

ADMM updates the variables $\tilde{\mathbf{x}}$, $\mathbf{v}$, and $\mathbf{u}$ in an alternating scheme. It splits the unrolled reconstruction into three steps, as shown in Equation (3). The updating step for $\tilde{\mathbf{x}}$ is solved by conjugate gradient, the variable $\mathbf{v}$ is then updated via the forward pass of the neural network $\mathcal{D}_\omega$ with the input as the sum of current estimates of $\tilde{\mathbf{x}}$ and $\mathbf{u}$, and eventually the variable $\mathbf{u}$ is updated based on current estimates of all variables.

The index k in Equation (3) denotes the unrolling iteration, and $\mathcal{D}_\omega$ denotes the residual network parameterized by ω.

C. Latent Space Embedded Zero-Shot Learning

ZSSSL partitions the undersampled data into three sets, so the sampling mask ($\mathbf{P}$) becomes $\mathbf{P} = \mathbf{P}_1 \cup \mathbf{P}_2 \cup \mathbf{P}_3$. Here, $\mathbf{P}_1$ is used for the data consistency term during training, which modifies the $\tilde{\mathbf{x}}$ update step in Equation (3) as $\tilde{\mathbf{x}}^{(k+1)} = \operatorname{argmin}_{\mathbf{x}} \|\mathbf{P}_1\mathbf{y} - \mathbf{P}_1\mathcal{A}(\mathbf{x})\|_2^2 + \rho/2 \left\|\mathbf{x} - \mathbf{v}^{(k)} + \mathbf{u}^{(k)}\right\|_2^2$. Given the estimated $\tilde{\mathbf{x}}$, $\mathbf{P}_2$ is then used to define the training loss function:

$$\mathcal{L}(\mathbf{P}_2\mathbf{y}, \mathbf{P}_2\mathcal{A}(\tilde{\mathbf{x}})) \tag{4}$$

which is computed from the mixed-ℓ^1-ℓ^2 norm of the two inputs [29]. $\mathbf{P}_3$ is used to compute the validation loss. When the validation loss is consecutively smaller than the training loss for 12 times, the training process will be stopped. After training, the undersampled data set is used for inference.

IV. Results

A. VAE enables robust & accurate learning of DWI signal

B. Zero-shot learning enables motion-robust DWI

C. Zero-shot learning: model generalization

D. VAE modeling with zero-shot learning reconstruction

V. Discussion

VI. Conclusion

References

[1] T. R. Brown, B. M. Kincaid, and K. Uğurbil, "NMR chemical shift imaging in three dimensions," *Proc. Natl. Acad. Sci. USA*, vol. 79, pp. 3532–3526, 1982.

[2] D. Le Bihan, E. Breton, D. Lallemand, P. Grenier, E. Cabanis, and M. Laval-Jeantet, "MR imaging of intravoxel incoherent motions: application to diffusion and perfusion in neurologic disorders," *Radiology*, vol. 161, pp. 401–407, 1986.

[3] K.-D. Merboldt, W. Hanicke, and J. Frahm, "Self-diffusion NMR imaging using stimulated echoes," *J. Magn. Reson.*, vol. 64, pp. 479–486, 1985.

[4] M. Doneva, P. Börnert, H. Eggers, C. Stehning, J. Sénégas, and A. Mertins, "Compressed sensing for magnetic resonance parameter mapping," *Magn. Reson. Med.*, vol. 64, pp. 1114–1120, 2010.

[5] D. Ma, V. Gulani, N. Seiberlich, K. Liu, J. L. Sunshine, J. L. Duerk, and M. A. Griswold, "Magnetic resonance fingerprinting," *Nature*, vol. 495, pp. 187–192, 2013.

[6] E. O. Stejskal and J. Tanner, "Spin diffusion measurements: Spin echoes in the presence of time-dependent field gradient," *J. Chem. Phys.*, vol. 42, pp. 288–292, 1965.

[7] P. Mansfield, "Multi-planar image formation using NMR spin echoes," *J Phys C*, vol. 10, pp. 55–58, 1977.

[8] P. B. Roemer, W. A. Edelstein, C. E. Hayes, S. P. Souza, and O. M. Mueller, "The NMR phased array," *Magn. Reson. Med.*, vol. 16, pp. 192–225, 1990.

[9] D. K. Sodickson and W. J. Manning, "Simultaneous acquisition of spatial harmonics (SMASH): Fast imaging with radiofrequency coil arrays," *Magn. Reson. Med.*, vol. 38, pp. 591–603, 1997.

[10] K. P. Pruessmann, M. Weiger, M. B. Scheidegger, and P. Boesiger, "SENSE: Sensitivity encoding for fast MRI," *Magn. Reson. Med.*, vol. 42, pp. 952–962, 1999.

[11] K. P. Pruessmann, M. Weiger, P. Börnert, and P. Boesiger, "Adcances in sensitivity encoding with arbitrary k-space trajectories," *Magn. Reson. Med.*, vol. 46, pp. 638–651, 2001.

[12] M. A. Griswold, P. M. Jakob, R. M. Heidemann, M. Nittka, V. Jellus, J. Wang, B. Kiefer, and A. Haase, "Generalized autocalibrating partially parallel acquisitions (GRAPPA)," *Magn. Reson. Med.*, vol. 47, pp. 1202–1210, 2002.

[13] M. Lustig, D. Donoho, and J. M. Pauly, "Sparse MRI: The application of compressed sensing for rapid MR imaging," *Magn. Reson. Med.*, vol. 58, pp. 1182–1195, 2007.

[14] K. T. Block, M. Uecker, and J. Frahm, "Undersampled radial MRI with multiple coils. Iterative image reconstruction using a total variation constraint," *Magn. Reson. Med.*, vol. 57, pp. 1186–1098, 2007.

[15] Z.-P. Liang, "Spatiotemporal imaging with partially separable functions," in *4th IEEE International Symposium on Biomedical Imaging: From Nano to Macro (ISBI'4)*, 2007, pp. 988–991.

[16] J.-F. Cai, E. J. Candès, and Z. Shen, "A singular value thresholding algorithm for matrix completion," *SIAM. J. Optim.*, vol. 20, pp. 1956–1982, 2010.

[17] C. Huang, C. G. Graff, E. W. Clarkson, A. Bilgin, and M. I. Altbach, "T_2 mapping from highly undersampled data by reconstruction of principal component coefficient maps using compressed sensing," *Magn. Reson. Med.*, vol. 67, pp. 1355–1366, 2012.

[18] F. Lam and Z.-P. Liang, "A subspace approach to high-resolution spectroscopic imaging," *Magn. Reson. Med.*, vol. 71, pp. 1349–1357, 2014.

[19] D. F. McGivney, E. Pierre, D. Ma, Y. Jiang, H. Saybasili, V. Gulani, and M. A. Griswold, "SVD compression for magnetic resonance fingerprinting in the time domain," *IEEE Trans. Med. Imaging*, vol. 33, pp. 2311–2322, 2014.

[20] J. I. Tamir, M. Uecker, W. Chen, P. Lai, M. T. Alley, S. S. Vasanawala, and M. Lustig, "T_2 shuffling: Sharp, multicontrast, volumetric fast spin-echo imaging," *Magn. Reson. Med.*, vol. 77, pp. 180–195, 2017.

[21] G. E. Hinton and R. R. Salakhutdinov, "Reducing the dimensionality of data with neural networks," *Science*, vol. 313, pp. 504–507, 2006.

[22] F. Lam, Y. Li, and X. Peng, "Constrained magnetic resonance spectroscopic imaging by learning nonlinear low-dimensional models," *IEEE Trans. Med. Imaging*, vol. 39, pp. 545–555, 2019.

[23] M. Mani, V. A. Magnotta, and M. Jacob, "qModeL: A plug-and-play model-based reconstruction for highly accelerated multi-shot diffusion MRI using learned priors," *Magn. Reson. Med.*, vol. 86, pp. 835–851, 2021.

[24] S. Boyd, N. Parikh, E. Chu, B. Peleato, and J. Eckstein, "Distributed optimization and statistical learning via the alternating direction method of multipliers," *Foundations and Trends in Machine Learning*, vol. 3, pp. 1–122, 2010.

[25] K. Gregor and Y. LeCun, "Learning fast approximations of sparse coding," in *27th International Conference on Machine Learning (ICML'27)*, 2010, pp. 399–406.

[26] V. Monga, Y. Li, and Y. C. Eldar, "Algorithm Unrolling: Interpretable, Efficient Deep Learning for Signal and Image Processing," *IEEE Signal Processing Magazine*, vol. 38, pp. 18–44, 2021.

[27] K. Hammernik, T. Klatzer, E. Kobler, M. P. Recht, D. K. Sodickson, T. Pock, and F. Knoll, "Learning a variational network for reconstruction of accelerated MRI data," *Magn. Reson. Med.*, vol. 79, pp. 3055–3071, 2018.

[28] H. K. Aggarwal, M. P. Mani, and M. Jacob, "MoDL: Model-based deep learning architecture for inverse problems," *IEEE Trans. Med. Imaging*, vol. 38, pp. 394–405, 2018.

[29] B. Yaman, S. A. H. Hosseini, S. Moeller, J. Ellermann, K. Uğurbil, and M. Akçakaya, "Self-supervised learning of physics-guided reconstruction neural networks without fully sampled reference data," *Magn. Reson. Med.*, vol. 84, pp. 3172–3191, 2020.

[30] B. Yaman, S. A. H. Hosseini, and M. Akçakaya, "Zero-shot self-supervised learning for MRI reconstruction," in *10th International Conference on Learning Representations (ICLR'10)*, 2022.

[31] F. Knoll, J. Zbontar, A. Sriram, M. J. Muckley, M. Bruno, A. Defazio, M. Parente, K. J. Geras, J. Katsnelson, H. Chandarana, Z. Zhang, M. Drozdzalv, A. Romero, M. Rabbat, P. Vincent, J. Pinkerton, D. Wang, N. Yakubova, E. Owens, C. L. Zitnick, M. P. Recht, D. K. Sodickson, and Y. W. Lui, "fastMRI: A Publicly Available Raw k-Space and DICOM Dataset of Knee Images for Accelerated MR Image Reconstruction Using Machine Learning," *Radiology: Artificial Intelligence*, vol. 2, p. e190007, 2020.

[32] F. Liu, R. Kijowski, G. E. Fakhri, and L. Feng, "Magnetic resonance parameter mapping using model-guided self-supervised deep learning," *Magn. Reson. Med.*, vol. 85, pp. 3211–3226, 2021.

[33] Y. Arefeen, J. Xu, M. Zhang, Z. Dong, F. Wang, J. White, B. Bilgic, and E. Adalsteinsson, "Latent signal models: Learning compact representations of signal evolution for improved time-resolved, multi-contrast MRI," *Magn. Reson. Med.*, vol. 90, pp. 483–501, 2023.

[34] P. J. Basser, J. Mattiello, and D. Le Bihan, "MR diffusion tensor spectroscopy and imaging," *Biophys. J.*, vol. 66, pp. 259–267, 1994.

[35] Z. Tan, P. A. Liebig, R. M. Heidemann, F. B. Laun, and F. Knoll, "Accelerated diffusion-weighted magnetic resonance imaging at 7 T: Joint reconstruction for shift-encoded navigator-based interleaved echo planar imaging (JETS-NAViEPI)," *Imaging Neuroscience*, vol. 2, pp. 1–15, 2024.

[36] D. P. Kingma and M. Welling, "Auto-encoding variational bayes," in *2nd International Conference on Learning Representations (ICLR'2)*, 2014.

[37] O. Ronneberger, P. Fischer, and T. Brox, "U-Net: Convolutional Networks for Biomedical Image Segmentation," in *18th International Conference on Medical Image Computing and Computer-Assisted Intervention (MICCAI'18)*, 2015, pp. 234–241.

[38] K. He, X. Zhang, S. Ren, and J. Sun, "Deep residual learning for image recognition," in *IEEE Conference on Computer Vision and Pattern Recognition (CVPR'16)*, 2016, pp. 770–778.

[39] A. Heydari, A. Ahmadi, T. H. Kim, and B. Bilgic, "Joint MAPLE: Accelerated joint T_1 and T_2^* mapping with scan-specific self-supervised networks," *Magn. Reson. Med.*, 2024.